European Journal of Radiology 85 (2016) 1174–1180

Contents lists available at ScienceDirect

European Journal of Radiology

journal homepage: www.elsevier.com/locate/ejrad

The effect of late-phase contrast enhancement on semi-automatic software measurements of CT attenuation and volume of part-solid nodules in lung adenocarcinomas

Julien G. Cohen[a,b], Jin Mo Goo[a,c,*], Roh-Eul Yoo[a], Su Bin Park[a], Bram van Ginneken[d], Gilbert R. Ferretti[b,e], Chang Hyun Lee[a], Chang Min Park[a,c]

[a] Department of Radiology, Seoul National University College of Medicine, and Institute of Radiation Medicine, Seoul National University Medical Research Center, Seoul, Republic of Korea
[b] Clinique Universitaire de Radiologie et Imagerie Médicale (CURIM), Université Joseph Fourier, Centre Hospitalier Universitaire de Grenoble, CS 10217, 38043 Grenoble Cedex 9, France
[c] Cancer Research Institute, Seoul National University College of Medicine, Seoul, Republic of Korea
[d] Department of Radiology and Nuclear Medicine, Radboud University Nijmegen Medical Center, Geert Grooteplein 10, 6525 GA Nijmegen, the Netherlands
[e] INSERM U 823, Institut A Bonniot, 38700 La Tronche, France

ARTICLE INFO

Article history:
Received 22 December 2015
Received in revised form 14 March 2016
Accepted 29 March 2016

Keywords:
Lung nodule
Solitary pulmonary nodule
Lung cancer
Subsolid nodule
Adenocarcinoma
Contrast media

ABSTRACT

Objectives: To evaluate the differences in semi-automatic measurements of CT attenuation and volume of part-solid nodules (PSNs) between unenhanced and enhanced CT scans.
Materials and methods: CT scans including unenhanced and enhanced phases (slice thickness 0.625 and 1.25 mm, respectively) for 53 adenocarcinomas presenting as PSNs in 50 patients were retrospectively evaluated. For each nodule, semi-automatic segmentation provided the diameter, mean attenuation, mass, and volume of a whole nodule and its solid component. Interscan variability and statistical significance of the differences in those measures according to the adenocarcinoma category were evaluated by one reader.
Results: All parameters except for the mean attenuation of the solid components, were significantly increased on enhanced CT ($p < 0.05$). For the whole nodule, the mean relative differences were as follows: the longest diameter, 1.4% (limits of agreement, −6.2–9.1); volume, 2.4% (−26.7–31.4); mass, 7.0% (−11.3–25.2); mean attenuation, 2.7% (−5.6–11). For the nodule's solid component, those differences were as follow: the longest diameter, 6.9% (−34.4–48.2); volume, 17.9% (−77.8–113.7); mass, 18.8% (−77.8–115.4). The differences of measures between the unenhanced and enhanced CT were not significantly different between two groups of adenocarcinoma in situ/minimally invasive adenocarcinomas and invasive adenocarcinomas ($p > 0.05$).
Conclusions: As most volumetric and attenuation measurements changed significantly after contrast enhancement, care should be taken in comparing unenhanced and enhanced CT in the evaluation of PSNs.

1. Introduction

CT diagnosis and characterization of persistent subsolid nodules has become an important issue owing to their increased detection and close association with lung adenocarcinoma [1,2]. In comparison with solid nodules, subsolid nodules consist of ground-glass components and solid components, typically representing lepidic growth patterns and invasive components of adenocarcinoma on histology, respectively. Therefore, in the Fleischner Society guidelines [2], the management of subsolid nodules is based on the categorization of nodules according to the size of whole nodules and their solid components. In addition to the size of nodules, the volume, mass, and attenuation of nodules are important measures in determining the growth of subsolid nodules [3]. Recently, semi-automated software has been used to obtain these measures and interscan variability of these parameters has been reported in previous studies [4–7].

* Corresponding author at: Department of Radiology, Seoul National University Hospital, 101 Daehak-ro, Jongno-gu, Seoul 110-744, Republic of Korea.
E-mail addresses: jmgoo@plaza.snu.ac.kr, jmgoo@snu.ac.kr (J.M. Goo).

http://dx.doi.org/10.1016/j.ejrad.2016.03.027
0720-048X/

Contrast enhancement has been used in the characterization of pulmonary nodules, and may artificially increase nodule volume compared with unenhanced scans in solid nodules [8–10]. On the other hand, the enhancement pattern of subsolid nodules has rarely been reported probably because of the relatively low cellularity of a tumor manifesting as a subsolid nodule [11]. Recently, a quantitative analysis of subsolid nodules obtained with dual-energy CT has demonstrated an added value of the iodine-enhanced imaging parameters in distinguishing invasive adenocarcinoma (IA) from adenocarcinoma in situ (AIS) or minimally invasive adenocarcinoma (MIA) [12]. However, although scanning parameters [13,14] as well as other factors such as lung inflation or gravity [15] are known to affect ground glass nodules' assessment, the effect of contrast enhancement on the various measurements of subsolid nodules, which may show considerable interscan variability between unenhanced and contrast-enhanced CT scans, has not been thoroughly evaluated.

Therefore, the purpose of our study was to assess the differences in the semi-automatic software measurements of both solid and ground-glass components between unenhanced and enhanced CT scans in lung adenocarcinomas presenting as part-solid nodules.

2. Material and methods

This study was approved by the Institutional Review Board of our institution, and written informed consent was waived in this retrospective study.

2.1. Patient selection

We retrospectively reviewed all preoperative CT scans for the part-solid ground-glass nodules (GGNs) with consecutive pre- and post-enhancement acquisitions between July 2014 and May 2015. Those studies were found using a picture archiving and communication system workstation (PACS) search specifying the corresponding CT protocol. Of 70 patients with 74 nodules found with the PACS search, we excluded 21 patients with 21 nodules for the following reasons: (1) no surgery (1 nodule in 1 patient), (2) reassessment as solid nodules at retrospective review (2 nodules in 2 patients), (3) masses rather than nodules with diameters greater than 3 cm (1 mass in 1 patient), (4) histopathologic diagnosis other than adenocarcinoma (4 nodules in 4 patients including 1 capillary hemangioma, 1 aspergilloma, 1 focal fibrosis, 1 non caseating granuloma), (5) inadequate segmentation (8 nodules in 8 patients—see segmentation paragraph for more details), and (6) pure GGNs (5 nodules in 4 patients). Finally, 53 part-solid nodules in 50 patients (20 men and 30 women; mean age, 62 years; age range, 34–77 years) were included in this study.

2.2. CT technique

CT images were obtained using GE Discovery 750CT scanner (GE Healthcare, Milwaukee, WI). The CT protocol consisted of an unenhanced scan followed by a contrast-enhanced scan: (1) a tube voltage of 120 kV with the tube current-time product determined automatically at a noise index of 70.44, and a reconstruction slice thickness of 0.625 mm for unenhanced acquisition; (2) a tube voltage of 120 kV with the tube current-time product determined automatically at a noise index of 22.67, and a reconstruction slice thickness of 1.25 mm for contrast-enhanced acquisition. Both CT examinations were scanned with a collimation of 64×0.625 mm, a pitch of 0.984 and reconstructed with the same bone kernel and with a FOV of 300–360 mm according the size of patients' thoracic cage. For all further processing, images were displayed with lung window settings (window width, 1500HU; level, −700HU).

With regard to the contrast administration, 70 mL (if the patient's weight is 60 kg or less) or 90 mL (if the patient's weight exceeds 60 kg) of a nonionic contrast medium (Pamiray 370; Dongkook Pharm., Seoul, Korea) was injected into the antecubital vein at 3 mL/s, followed by 30 mL of normal saline at the same flow rate, by using a dual power injector (Stellant; Medrad, Indianola, PA). Data acquisition was started after a delay of 60 s (late phase). The estimated time interval between unenhanced and enhanced scans was less than 3 min for each patient and the patient's position was not changed between the two scans.

Images were transferred to the workstation equipped with Quad Core CPU and 16 GB memory for further analysis.

2.3. Image analysis

Unenhanced and enhanced acquisitions for each nodule were segmented with Veolity software (version 1.1, MeVis Medical Solutions, Bremen, Germany) by one radiologist with 4 years of experience (J.C.). The software has been shown to be capable of segmenting ground-glass and solid components in GGNs with accuracy at least as good as expert radiologists [6]. After the targeting of nodules, the software enabled automatic segmentation of their ground-glass and solid components, providing for each of them the largest diameter, volume, mass and attenuation. Mass was calculated by the software using the segmented nodule's volume and mean attenuation using the formula previously described by de Hoop et al. [16]. Subsequently, further adjustments were allowed to be made if needed by the same radiologist who processed the segmentation, including modifications in lower attenuation thresholds for solid and ground-glass components, placement of seed points, and lesion roundness. In this study, thresholds of −750HU and −350HU were used by default for ground-glass components and solid components of all nodules, respectively. However, further adjustments of those thresholds, in addition to lesion roundness and seed points, were allowed when the segmentation proposed by software was inadequate on at least one of the two acquisitions available for each nodule (see segmentation paragraph).

2.4. Software segmentation

We classified the segmentation results according to the previously reported criteria [17]: (1) excellent segmentation of both GGN and solid components, (2) good segmentation in which the proportion of correct segmentation was 80% or greater (subjective assessment) for both components with no vessel incorrectly segmented as a solid component, (3) insufficient segmentation in which the proportion was less than 80% for either component (subjective assessment) or a vessel was incorrectly segmented as a solid component, (4) failure in which a nodule could not be segmented or the result was completely inadequate when compared with visual assessment. If the segmentation results were different between the unenhanced and enhanced acquisitions, worse segmentation score was recorded. Segmentation scores were then further classified into two groups: adequate segmentation (1 and 2) and inadequate segmentation (3 and 4).

When segmentation was inadequate using default values, manual adjustments were applied for the following parameters: lower attenuation thresholds, lesion roundness, and seed points. Such adjustments proved to have no direct influence on interscan variability in a previous study using the same software [6]. Nodules with persistently inadequate segmentation after adjustments were excluded (8 nodules in 8 patients).

2.5. Surgery and pathology

Of the 53 nodules included in the final analysis, 26 were resected by lobectomy and 27 by sublobar resection (12 by segmentectomy and 15 by wedge resection).

The 53 nodules corresponded pathologically to 1 AIS, 11 MIA and 41 IA.

3. Statistics

In this study we tested the null hypothesis that there is no difference between unenhanced and enhanced CT scans in the semi-automatic measurements of part-solid nodules.

Differences between unenhanced and enhanced acquisitions were evaluated using the Bland-Altman method [18] for the following parameters: the longest transverse diameter, mean attenuation, volume, and mass for both whole nodules and their solid components. Bland-Altman's mean differences and limits of agreement were reported as both absolute and relative differences. The absolute difference referred to the actual difference in the parameters between unenhanced and enhanced scans. The relative difference was the percent difference in the parameters calculated using the following formula:

$$\textit{Relative Difference}\,(\%) = \frac{V2 - V1}{|0.5 * (V1 + V2)|} * 100$$

, where V1 and V2 are values of the parameters on unenhanced and enhanced scans, respectively. Limits of agreement for both absolute and relative differences were defined as the 95% confidence intervals of the mean differences.

An additional analysis using the Wilcoxon signed rank test was performed for the parameters in order to determine differences between enhanced and unenhanced scans on a group level. Statistical significance of differences between unenhanced and enhanced scans according to the adenocarcinoma category was evaluated with the Wilcoxon rank-sum test. For this comparison, AIS and MIA were categorized together, given the similar prognosis and management of the nodules [19]. Non-parametric tests were chosen since tested parameters did not have normal distributions.

All statistical analyses were performed with R software (Version 3.2.0; http://www.r-project.org/). Results with P values less than 0.05 were considered statistically significant.

4. Results

4.1. Software segmentation

Among the 61 nodules initially included in the analysis, 53 were adequately segmented (52 perfect segmentation, 1 good segmentation). Of those 53 nodules, adjustments after initial segmentation were applied in 26 nodules (49%). An example of adequate nodule segmentation is given in Fig. 1.

Adequate segmentation could not be obtained for both unenhanced and enhanced CT scans in 8 nodules. Specific causes for inadequate segmentation were as follows: (1) the presence of bubble-like lucency within the ground-glass component (n = 1), (2) faint ground-glass component (n = 1), (3) partial segmentation of the chest wall (n = 3), (4) misclassification of a blood vessel as the solid component (n = 2), and (5) surrounding dependent opacity (n = 1).

4.2. CT findings

The mean longest diameter of whole nodule and part-solid component of included nodules were of 14.8 and 7.4 mm, and 15 and 7.7 mm for unenhanced and enhanced studies, respectively. Nodules were found in the right upper lobe in 23 cases (43%), right middle lobe in 3 cases (6%), right lower lobe in 11 cases (21%), left upper lobe in 9 cases (17%), and left lower lobe in 7 cases (13%).

4.3. Differences between unenhanced and enhanced CT scans

Absolute and relative differences as well as their limits of agreement with the Bland-Altman method are given in Table 1. Corresponding Bland-Altman curves for the relative difference are shown in Fig. 2.

4.3.1. Longest diameter

The longest transverse diameters of both the whole nodules and solid components were significantly increased after contrast injection ($p < 0.05$) with the mean absolute difference of 0.19 mm (limits of agreement, −0.74–1.11) and the mean relative difference of 1.4% (−6.2–9.1) for the whole nodules and 0.29 mm (−1.16–1.73) and 6.9% (−34.4–48.2) for the solid components.

4.3.2. Volume and mass measurement

The volume and mass of the whole nodules were significantly higher on enhanced CT scans ($p < 0.05$), with limits of agreement ranging from −26.7% to 31.4% (mean relative difference, 2.4%) for the volume measurements and from −11.3% to 25.2% (mean relative difference, 7.0%) for the mass measurements. The volume and mass of the solid components were also significantly higher on enhanced CT scans ($p < 0.05$) with limits of agreement ranging from −77.8% to 113.7% for the volume measurements and from −77.8% to 115.4% for the mass measurements.

4.3.3. Attenuation

There was a significant increase in the mean attenuation of the whole nodules after contrast injection with a mean increase in the overall nodule attenuation of 13.8HU (limits of agreement, −27.7–55.3). However, the mean attenuations of the solid components were not significantly different between unenhanced and enhanced scans ($p > 0.05$).

4.4. Differences of measures between unenhanced and enhanced scans according to the adenocarcinoma category

Differences in various measures of the whole nodules and the solid components (i.e., the longest diameter, volume, mass, and attenuation) between unenhanced and enhanced scans did not significantly differ between AIS/MIA group and IA group ($p > 0.05$) (Table 2).

5. Discussion

Determining the optimal management for incidentally or screening-detected nodules is often challenging because of their small sizes, and in particular, the recognition of changes in various measures of the nodules is crucial in assessing their malignancy risk, which is a key determinant of their management [3]. In addition to the size and volume which are used in the evaluation of solid nodules, the mass and attenuation are also reported to be effective measures in the evaluation of subsolid nodules. For the accurate assessment of changes in the measures, understanding the potential sources of measurement variability is important especially when dealing with subsolid nodules which typically show slow growth rates [20].

Although it is recommended to use the same CT protocols when comparing nodules, we frequently compare CT scans obtained within different protocols in routine practice. In this study, we attempted to evaluate the effect of contrast enhancement on the

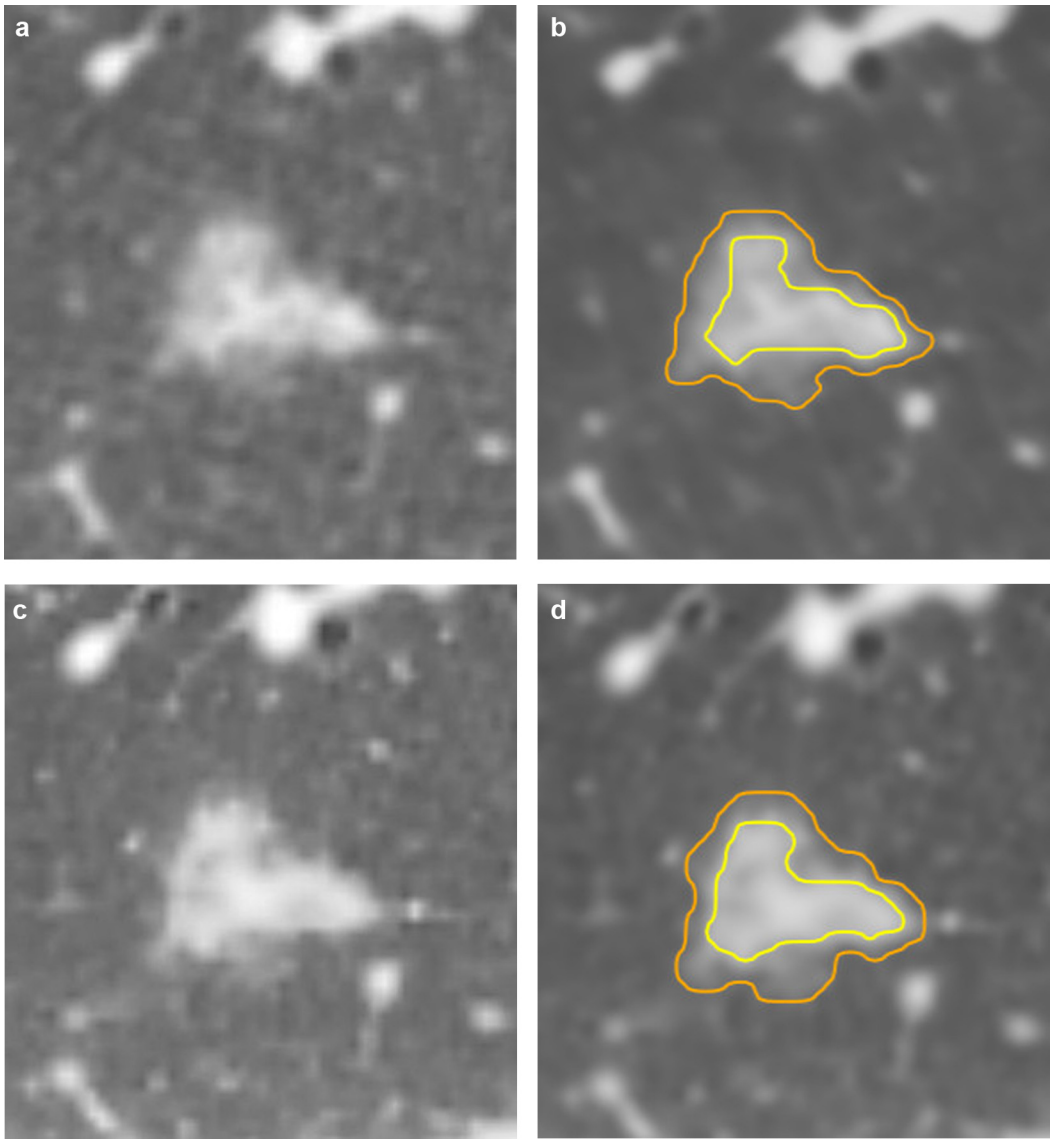

Fig. 1. Unenhanced (A and B) and enhanced (C and D) CT scans displayed with lung window (window width, 1500HU; level, −700HU) show a subsolid nodule in a 63 year-old female patient which was confirmed as minimally invasive adenocarcinoma. Orange boundaries on B and D indicate borders of the whole nodule, while yellow boundaries indicate borders of the solid component. The largest diameter, volume, mass, and attenuation of the whole nodule was greater on enhanced CT scan (13.1 mm, 1164 mm^3, 633 mg, 456HU) than on unenhanced CT scan (12.5 mm, 1026 mm^3, 552 mg, 462HU).

Table 1
CT measures of part-solid nodules on unenhanced and enhanced scans (n = 53).

CT measures	Unenhanced scan[a]	Enhanced scan[a]	Mean absolute difference[b]	Mean relative difference[a]	p-value
Longest diameter, whole nodule (mm)	14.8 [6.5; 24.7]	15.0 [6.7; 25.4]	0.19 [−0.74; 1.11]	1.4% [−6.2; 9.1]	**< 0.001**
Longest diameter, solid component (mm)	7.4 [0.8; 15]	7.7 [1.1; 15.2]	0.29 [−1.16; 1.73]	6.9% [−34.4; 48.2]	**0.002**
Volume, whole nodule (mm^3)	2199.3 [146.2; 7931]	2260.1 [157.6; 8628.7]	60.8 [−377.5; 499.1]	2.4% [−26.7; 31.4]	**0.03**
Volume, solid component (mm^3)	410.3 [0.3; 1758.4]	426.0 [0.7;1848.6]	17.9 [−194.7; 227.4]	17.9% [−77.8; 113.7]	**0.003**
Mass, whole nodule (mg)	1091.8 [55.8; 3406.8]	1159.8 [65.3; 3778.7]	68.0 [−129.5; 265.6]	7.0% [−11.3; 25.2]	**< 0.001**
Mass, solid component (mg)	344.2 [0.2; 1521.3]	359.2 [0.5; 1593.5]	15.0 [−161.6; 191.6]	18.8% [−77.8; 115.4]	**0.004**
Mean attenuation, whole nodule (HU)	−527.6 [−671.8; −361.4]	−515.8 [−642.8; −363.4]	13.8 [−27.7; 55.3]	2.7% [−5.6; 11]	**< 0.001**
Mean attenuation, solid component (HU)	−195.6 [−315.7; 120.3]	−191.8 [−314.4; 152.2]	3.8 [−41.6; 49.1]	2.3% [−20.2; 24.7]	0.20

Differences in the measures were evaluated using the Wilcoxon's signed rank test.
[a] Data are given as mean with minimal and maximal values.
[b] Values are given with their limits of agreements according to Bland-Altman method, defined as the 95% CIs of the difference.

measurements of subsolid nodule on CT scans obtained in a short time interval without positional changes of patients, provided that there is currently no evidence that nodule parameters obtained on unenhanced and enhanced scans are comparable in adenocarcinomas manifesting as subsolid nodules.

In our study, measures of all parameters for both whole nodules and their solid components were found to be significantly higher on contrast-enhanced scans except for mean attenuation of the solid components. The significant increases in the mean attenuation and mass for the whole nodules could be expected, given that

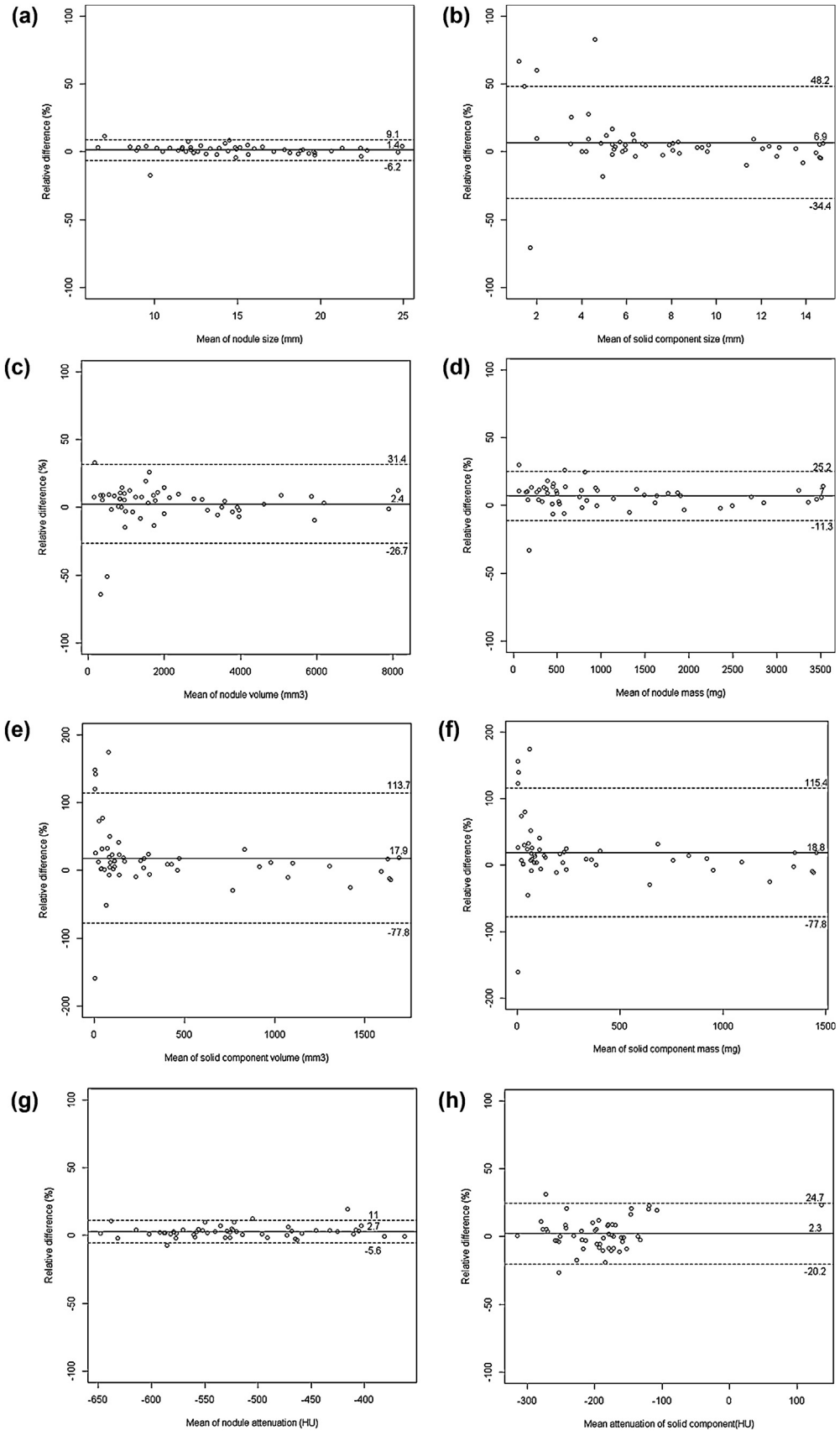

Fig. 2. Bland-Altman plots for relative differences of the values for each parameter of whole nodule and solid component between unenhanced and enhanced scans.

Table 2
Differences in CT measures between unenhanced and enhanced scans according to the adenocarcinoma category.

CT measures	Mean difference in AIS/MIA[a] (n = 12)	Mean difference in IA[a] (n = 41)	p-value[a]
Longest diameter, whole nodule (mm)	0.23 [0.01; 0.46]	0.17 [0.03; 0.33]	0.64
Longest diameter, solid component (mm)	0.31 [−0.05; 0.66]	0.28 [0.03; 0.53]	0.39
Volume, whole nodule (mm^3)	−2.71 [−72.3; 66.8]	79.4 [1.99; 156.8]	0.19
Volume, solid component (mm^3)	15.3 [1.1; 29.4]	16 [−22.5; 54.4]	0.61
Mass, whole nodule (mg)	31.7 [9.6; 53.7]	78.7 [43.6; 113.8]	0.15
Mass, solid component (mg)	13.1 [1.4; 24.8]	15.5 [−16.8; 47.8]	0.75
Mean attenuation, whole nodule (HU)	15.3 [4.9; 25.6]	13.4 [6.2; 20.5]	0.68
Mean attenuation, solid component (HU)	6.0 [−14.6; 26.6]	3.1 [−3.2; 9.5]	0.98

Differences in the measures were evaluated using the Wilcoxon's rank sum test.
[a] Values of the mean differences are given with their 95% CIs.

nodule attenuation increases after contrast enhancement. However, the mean attenuation of the solid components, although slightly increased on average on enhanced studies, showed no significant difference between the two scans. That absence of significance could be explained by several reasons: first, due to the small size of the solid component, there was significant variability of its attenuation measurement with possible partial volume effects, added to the fact that the observed average enhancement was quite small (i.e., average attenuations of −192 and −196 HU for enhanced and non-enhanced studies respectively); second, in our study, measurements were performed on images reconstructed bone kernel only, which may also reduce the sensitivity of the detection of such a small enhancement. Regarding the mass of the whole nodules, its interscan variability in our study was similar to the limits of agreement reported on unenhanced CT scans by Kim et al. (i.e., −17.7–18.8%) [21], but slightly lower than those reported by Scholten et al. (i.e., −27.6–30.8%) [6]. Overall, according to these results, the variability of mass between unenhanced and enhanced scans was therefore comparable to or lower than the that between different unenhanced scans, probably because there was no position change in our study.

With regard to the sizes and volumes for both whole nodules and solid components after contrast administration, several factors may have contributed to their significant increases after contrast administration. The effect of contrast injection on nodule volume estimated by semi-automatic segmentation was previously described in solid nodules by several authors: Honda et al. [9] and Rampinelli et al. [10], who compared semi-automated nodule volumetry before and after injection in 60 and 35 solid nodules respectively, found that the volume was significantly increased after injection, with volume increases ranging between 4 and 9%. De Jong et al. [8] reported similar results when comparing low-dose unenhanced CTs and non-low dose enhanced CT scans. We speculated that the volume change after contrast enhancement may be attributable to modification of semi-automatic segmentation margins as a result of the change in contrast between nodule edges and adjacent parenchyma. Indeed, the attenuation of lung parenchyma does increase after contrast medium injection and the degree of enhancement of this physiological enhancement and that of a nodule can be different. The differential of attenuation between nodule and parenchyma is therefore modified after injection, which results in segmentation differences. Similar variations have been reported with changes in the lung volume, which, in turn, causes changes in the background lung attenuation [22]. In our study, we need to point out that different scanning parameters between unenhanced and enhanced studies could also affect segmentation results. Indeed, the higher slice thickness on enhanced studies potentially creates more partial volume effect, and a lower noise index can also slightly modify recorded attenuation differentials.

Interestingly, our results pertaining to interscan variability of the longest diameter and volume were similar to those of the previous study focusing on unenhanced CTs (i.e., limits of agreements of −2–9%, and −35.4–8.6% for the longest diameter and volume, respectively), which may imply that contrast enhancement is only one of the factors responsible for those differences. Meanwhile, other authors reported lower limits of agreement for volume measurements on unenhanced CTs. Specifically, Park et al. reported limits of agreement of −18.6–18.9% on a series of 30 pure GGNs with consecutive acquisitions at a 10-minute interval [5]. Oda et al. reported limits of agreement of −16.6–15.7% on a series of 59 pure and part-solid nodules [4], and Kim et al. reported limits of agreement of −11.7–18.1% on a series of 94 pure and part-solid nodules [21].

In terms of the pathology, changes in measures for each parameter after contrast enhancement did not significantly differ between AIS/MIA and IA ($p > 0.05$). However, there was only one AIS in our study, and therefore the difference between AIS/MIA group and IA group may have been underestimated. Furthermore, only a single post-enhancement acquisition was studied in this study and dynamic CT at several time-points after injection may possibly provide more information.

There are several limitations in our study. First, inclusion of only surgically resected lesions may have resulted in a selection bias, because the prevalence of invasive lesions may be higher in the sample group than in the general population of GGNs. However, the CT-protocol used in this study, including unenhanced and enhanced scans obtained consecutively during the same exam, was exclusively performed in patients in a pre-operative state and differences related to pathology were also an important issue to assess. Second, slight differences in specific parameters of the CT protocol may have been responsible for some variations observed in this study, and these differences may have caused different segmentation results by semi-automatic approaches. Indeed, slice thickness differed slightly between unenhanced and enhanced studies (0.625 mm and 1.25 mm, respectively). However, both of those thicknesses are acceptable for the evaluation of GGNs. Third, while the volume of injected contrast media depended on patients' weight, the relationship was not linear as there were only two different volumes used in our protocol (i.e., 70 mL or 90 mL). Fourth, some biases may be due to the technique of semi-automatic segmentation. A single software was used, which may of course limit generalization to other software packages. Also, while the use of manual adjustments improves the quality of segmentation, it may increase interobserver variability, which was not analyzed in this particular study.

In conclusion, as most volumetric and attenuation measurements changed significantly after contrast enhancement, care should be taken in comparing unenhanced and enhanced CT scans in the evaluation of part-solid nodules.

Funding

This study was supported by a grant from the National R&D Program for Cancer Control, Ministry for Health and Welfare, Republic of Korea (1520230). The funding source had no involvement in study design; in the collection, analysis and interpretation of data; in the writing of the report; and in the decision to submit the paper for publication.

Conflict of interest

Professor Bram van Ginneken is affiliated with Fraunhofer MeVis, Bremen, Germany, and the remaining authors have no conflicts of interest.

Acknowledgements

J.C. acknowledges support from the Société Francaise de Radiologie (SFR) and Collège des Enseignants de Radiologie de France (CERF).

Appendix A. Supplementary data

Supplementary data associated with this article can be found, in the online version, at http://dx.doi.org/10.1016/j.ejrad.2016.03.027.

References

[1] J.M. Goo, C.M. Park, H.J. Lee, Ground-glass nodules on chest CT as imaging biomarkers in the management of lung adenocarcinoma, AJR Am. J. Roentgenol. 196 (2011) 533–543.
[2] D.P. Naidich, A.A. Bankier, H. MacMahon, et al., Recommendations for the management of subsolid pulmonary nodules detected at CT: a statement from the Fleischner Society, Radiology 266 (2013) 304–317.
[3] H. Kim, C.M. Park, J.M. Goo, J.E. Wildberger, H.U. Kauczor, Quantitative computed tomography imaging biomarkers in the diagnosis and management of lung cancer, Invest. Radiol. 50 (2015) 571–583.
[4] S. Oda, K. Awai, K. Murao, et al., Computer-aided volumetry of pulmonary nodules exhibiting ground-glass opacity at MDCT, AJR Am. J. Roentgenol. 194 (2010) 398–406.
[5] C.M. Park, J.M. Goo, H.J. Lee, K.G. Kim, M.J. Kang, Y.H. Shin, Persistent pure ground-glass nodules in the lung: interscan variability of semiautomated volume and attenuation measurements, AJR Am. J. Roentgenol. 195 (2010) W408–414.
[6] E.T. Scholten, P.A. de Jong, C. Jacobs, et al., Interscan variation of semi-automated volumetry of subsolid pulmonary nodules, Eur. Radiol. 25 (2015) 1040–1047.
[7] E.T. Scholten, C. Jacobs, B. van Ginneken, et al., Detection and quantification of the solid component in pulmonary subsolid nodules by semiautomatic segmentation, Eur. Radiol. 25 (2015) 488–496.
[8] P.A. de Jong, T. Leiner, J.W. Lammers, H.A. Gietema, Can low-dose unenhanced chest CT be used for follow-up of lung nodules, AJR Am. J. Roentgenol. 199 (2012) 777–780.
[9] O. Honda, T. Johkoh, H. Sumikawa, et al., Pulmonary nodules: 3D volumetric measurement with multidetector CT–effect of intravenous contrast medium, Radiology 245 (2007) 881–887.
[10] C. Rampinelli, S. Raimondi, M. Padrenostro, et al., Pulmonary nodules: contrast-enhanced volumetric variation at different CT scan delays, AJR Am. J. Roentgenol. 195 (2010) 149–154.
[11] W.D. Travis, E. Brambilla, M. Noguchi, et al., International association for the study of lung cancer/american thoracic society/european respiratory society international multidisciplinary classification of lung adenocarcinoma, J. Thorac. Oncol. 6 (2011) 244–285.
[12] J.Y. Son, H.Y. Lee, J.H. Kim, et al., Quantitative CT analysis of pulmonary ground-glass opacity nodules for distinguishing invasive adenocarcinoma from non-invasive or minimally invasive adenocarcinoma: the added value of using iodine mapping, Eur. Radiol. 26 (2016) 43–54.
[13] J.M. Goo, T. Tongdee, R. Tongdee, K. Yeo, C.F. Hildebolt, K.T. Bae, Volumetric measurement of synthetic lung nodules with multi-detector row CT: effect of various image reconstruction parameters and segmentation thresholds on measurement accuracy, Radiology 235 (2005) 850–856.
[14] E. Linning, M. Daqing, Volumetric measurement pulmonary ground-glass opacity nodules with multi-detector CT: effect of various tube current on measurement accuracy—a chest CT phantom study, Acad. Radiol. 16 (2009) 934–939.
[15] G.R. Ferretti, F. Arbib, J.F. Roux, V. Bland, S. Lantuejoul, Effect of lung volume and gravity on the attenuation and size of a pure ground-glass nodule, J. Thorac. Imaging 27 (2012) W15–17.
[16] B. de Hoop, H. Gietema, S. van de Vorst, K. Murphy, R.J. van Klaveren, M. Prokop, Pulmonary ground-glass nodules: increase in mass as an early indicator of growth, Radiology 255 (2010) 199–206.
[17] B. de Hoop, H. Gietema, B. van Ginneken, P. Zanen, G. Groenewegen, M. Prokop, A comparison of six software packages for evaluation of solid lung nodules using semi-automated volumetry: what is the minimum increase in size to detect growth in repeated CT examinations, Eur. Radiol. 19 (2009) 800–808.
[18] J.M. Bland, D.G. Altman, Statistical methods for assessing agreement between two methods of clinical measurement, Lancet 1 (1986) 307–310.
[19] P.E. Van Schil, H. Asamura, V.W. Rusch, et al., Surgical implications of the new IASLC/ATS/ERS adenocarcinoma classification, Eur. Respir. J. 39 (2012) 478–486.
[20] Y.S. Song, C.M. Park, S.J. Park, S.M. Lee, Y.K. Jeon, J.M. Goo, Volume and mass doubling times of persistent pulmonary subsolid nodules detected in patients without known malignancy, Radiology 273 (2014) 276–284.
[21] H. Kim, C.M. Park, S. Woo, et al., Pure and part-solid pulmonary ground-glass nodules: measurement variability of volume and mass in nodules with a solid portion less than or equal to 5 mm, Radiology 269 (2013) 585–593.
[22] J.M. Goo, K.G. Kim, D.S. Gierada, M. Castro, K.T. Bae, Volumetric measurements of lung nodules with multi-detector row CT: effect of changes in lung volume, Korean J. Radiol. 7 (2006) 243–248.